Oxovanadium(V) Alkoxo-Chloro Complexes of the Hydridotripyrazolylborates as Models for the Binding Site in Bromoperoxidase

Carl J. Carrano,*,† Madan Mohan,† Stephen M. Holmes,† Roger de la Rosa,‡ Alison Butler,‡ John M. Charnock,§ and C. David Garner§

Department of Chemistry, Southwest Texas State University, San Marcos, Texas 78666, Department of Chemistry, University of California, Santa Barbara, California 93106, and Department of Chemistry, University of Manchester, Oxford Road, Manchester, U.K. M13 9PL

Received March 30, 1993®

Vanadium(III) and -(V) alkoxo complexes of the ligands hydridotripyrazolylborate, L, and hydridotris(3,5-dimethylpyrazolyl)borate, L*, have been prepared and characterized by X-ray diffraction, ^{1}H, ^{13}C, and ^{51}V NMR, electrochemistry, optical spectroscopy, and EXAFS. Two general classes of V(V) complexes have been synthesized with the general formulas $LVO(OR)_2$ and LVO(OR)Cl. The latter complexes contain the shortest V–OR bonds yet reported (1.706–1.754 Å) and show that a vanadium–alkoxide bond could account for the short vanadium "light atom" interaction seen in the EXAFS of the enzyme, bromoperoxidase. The alkoxides undergo facile hydrolysis to yield a variety of oxo-bridged multinuclear species. One of these has been characterized by X-ray crystallography as the cyclic tetramer $[LVO_2]_4$. Crystallographic parameters for complexes prepared in this study: L*V(Cl)-OMe(DMF)·CH_2Cl_2, **I** ($C_{20}H_{34}BCl_3N_7O_2V$), MW = 572.6, a = 17.189(2) Å, b = 10.039(2) Å, c = 16.618(3) Å, β = 103.039(12)°, V = 2793.9(8) Å^3, monoclinic ($P2_1/c$), Z = 4; LVO(O-Pr^i))Cl, **V** ($C_{12}H_{17}BClN_6O_2V$), MW = 374.5, a = 13.361(3) Å, b = 14.583(3) Å, c = 18.016(4) Å, V = 3510.2(13) Å^3, orthorhombic ($Pbca$), Z = 8; LVO(O-Bu^t)Cl, **VI** ($C_{13}H_{19}BClN_6O_2V$), MW = 388.5, a = 12.783(3) Å, b = 15.312(3) Å, c = 18.843(4) Å, V = 3688.1(14) Å^3, orthorhombic ($Pbca$), Z = 8; L*VO(O-Bu^t)Cl, **X** ($C_{19}H_{30}BClN_6O_2V$), MW = 471.7, a = 8.619(2) Å, b = 17.761(4) Å, c = 16.139(3) Å, β = 104.58(3), V = 2389.9(9) Å^3, monoclinic ($P2_1/n$), Z = 4; $[LVO_2]_4$·$2CH_2Cl_2$·$2H_2O$, **XI** ($C_{38}H_{44}B_4Cl_4N_{24}O_{10}V_4$), MW = 1385.8, a = 15.634(3) Å, b = 16.202(3) Å, c = 24.406(5) Å, V = 6182(2) Å^3, orthorhombic ($Pccn$); Z = 4.

Introduction

For some time we have been engaged in studying vanadium complexes of the tripyrazolylborate ligand as models for vanadium histidine interactions which could exist in metalloproteins such as "bromoperoxidase."[1-3] This vanadium(V)-dependent enzyme is widely distributed in red and brown marine algae and catalyzes the reaction[4,5]

$$RH + H_2O_2 + Br^- \rightarrow RBr + H_2O + OH^-$$

A wide variety of physiochemical techniques indicate that the V(V) center is in an oxygen/nitrogen rich environment.[6,7] Based extensively on EXAFS analysis, a model for the active site has been proposed.[8] In this model the V(V) is coordinated to two nitrogen or oxygen atoms at 2.11 Å and three oxygen donors at 1.72 Å along with the ubiquitous oxo group at 1.61 Å. A similar environment has been suggested for the inactive, reduced enzyme containing V(IV). The primary difference between the two metal centers appears to be a lengthening of the V–O bond from the unknown oxygen donor from 1.72 to 1.91 Å. There has been considerable speculation as to the nature of the unknown oxygen donors, with the phenolate of tyrosine, carboxylates from glutamic or aspartic acid, or the deprotonated alcohol of a serine or threonine all being considered. Of the possible donors, the absence of characteristic LMCT bands in the optical spectrum of the enzyme would seem to preclude a tyrosine phenol, while carboxylates from glutamic or aspartic acid seem unlikely to give a V–O bond as short as 1.72 Å.[2,9,10] This leaves the deprotonated alcohols of serine or threonine as the only candidate ligands. However, several groups have suggested that the oxygen donors do not come from the protein at all but in fact represent protonated oxo groups on the vanadium center.[2,10] In order to investigate both of these possibilities more closely we have begun to examine alkoxy and hydroxy complexes of vanadium in all three of its biologically accessible oxidation states with the trispyrazolylborate, L, and tris(3,5-dimethylpyrazolyl)borate, L*, moieties. The tripyrazolylborate group was chosen as it provides a stable, facially coordinating platform with nitrogen donors that resemble those of the imidazole side chain of histidine. The results of these studies are reported herein.

Experimental Section

Materials. Unless otherwise stated, reactions were carried out under an atmosphere of pure dry argon or nitrogen by utilizing standard Schlenk techniques. Solvents were dried and distilled under a blanket of inert gas before use.

Potassium hydridotripyrazolylborates were prepared as previously described and their purity checked by proton NMR spectroscopy.[11,12]

† Department of Chemistry, Southwest Texas State University.
‡ Department of Chemistry, University of California, Santa Barbara.
§ Department of Chemistry, University of Manchester.
® Abstract published in *Advance ACS Abstracts,* January 1, 1994.

(1) Kime-Hunt, E.; Spartalian, K.; DeRusha, M.; Nunn, C. M.; Carrano, C. J. *Inorg. Chem.* **1989**, *28*, 4392.
(2) Holmes, S.; Carrano, C. J. *Inorg. Chem.* **1991**, *30*, 1231.
(3) Mohan, M.; Holmes, S. M.; Butcher, R. J.; Jasinski, J. P.; Carrano, C. J. *Inorg. Chem.* **1992**, *31*, 2031.
(4) Vilter, H. *Phytochemistry* **1984**, *23*, 1387.
(5) Wever, R.; de Boer, E.; Plat, H.; Krenn, B. E. *FEBS Lett.* **1987**, *216*, 1 and references therein.
(6) (a) de Boer, E.; Boon, K.; Weaver, R. *Biochemistry* **1988**, *27*, 1629. (b) de Boer, E.; Keijzers, C. P.; Klaassen, A. K.; Reijere, E. J.; Collison, D.; Garner, C. D.; Wever, R. *FEBS Lett.* **1988**, *235*, 93.
(7) Hormes, J.; Kuetgens, Chauvistre, R.; Schreiber, W.; Anders, N.; Vilter, H.; Rehder, D.; Weidemann, C. *Biochim. Biophys. Acta* **1988**, *956*, 293.
(8) Arber, J. M.; de Boer, E.; Garner, C. D.; Hasnain, S. S.; Wever, R. *Biochemistry* **1989**, *28*, 7968.
(9) Rehder, D.; Priebsch, W.; Oeynhausen, M. *Angew. Chem., Int. Ed. Engl.* **1989**, *28*, 1221.
(10) Li, X.; Lah, M. S.; Pecoraro, V. L. *Inorg. Chem.* **1988**, *27*, 4657.

0020-1669/94/1333-0646$04.50/0

Anhydrous vanadium trichloride and $VOCl_3$ were obtained from Aldrich Chemical Co. and used as received. $L^*VCl_2(DMF)$ and $L^*VO(Cl)$-DMF were synthesized according to published reports.[1]

Synthesis. [{HB(3,5-Me$_2$pz)$_3$}VCl(OCH$_3$)DMF], I and [{HB(3,5-Me$_2$pz)$_3$}V(OCH$_3$)$_2$]·H$_2$O, II. A slurry of excess $NaOCH_3$ was added to 0.53 g of [{HB(3,5-Me_2pz)$_3$}VCl_2DMF] in 20 mL of dry degassed toluene with constant stirring. The initially green solution darkened to a blue-violet color. The solution was allowed to stir overnight, filtered through Celite, and dried under vacuum. Crystallization of the dark purple residue from methylene chloride/hexane produced a crop of mixed crystals, which were hand separated. The purple crystals of the monosubstituted product **I** predominated. The violet crystal used for X-ray analysis was mounted directly from the mother liquor and proved to be the CH_2Cl_2 solvate. Samples sent for analysis were dried under vacuum and were thus desolvated. Blue crystals of what proved to be the monohydrate of the disubstituted product could also be isolated in small amounts.

Anal. Calcd for $C_{19}H_{32}N_7BO_2BCl$: C, 46.82; H, 6.57; N, 20.12. Found: C, 46.21; H, 6.57; N, 20.23.

Anal. Calcd for $C_{17}H_{28}N_6BO_2V·H_2O$: C, 47.66; H, 7.01; N, 19.63. Found: C, 47.41; H, 6.94; N, 19.44.

[{HB(pz)$_3$}VOCl(OR)] (R = Me, Et, Pr^i, Bu^t), III–VI. A solution of the predried alcohol, (3 Å molecular sieves, 0.02 mol in 10 mL of pentane) was added, with constant stirring, to a solution of $VOCl_3$ (0.02 mol) in 30 mL of pentane. The mixture was stirred for half an hour and the volatiles removed *in vacuo* to leave a viscous dark red liquid. The residue was redissolved in 30 mL of pentane, solid K[HB(pz)$_3$] (0.02 mol) was added, and the mixture was stirred for 1 h. The complex that precipitated was filtered off and dried under vacuum at room temperature. The resulting red material was dissolved in dichloromethane, filtered through Celite, and concentrated via rotary evaporation. Allowing the solution to stand afforded orange-red crystals of the desired complexes; average yield 75%.

Anal. Calcd for $C_{10}H_{13}N_6BO_2VCl·{}^1/_2H_2O$: C, 33.80; H, 3.94; N, 23.66. Found: C, 33.66; H, 3.75; N, 23.96.

Anal. Calcd for $C_{12}H_{17}N_6BO_2VCl$: C, 38.46; H, 4.54; N, 22.43. Found: C, 38.30; H, 4.46; N, 22.66.

Anal. Calcd for $C_{13}H_{19}N_6BO_2VCl$: C, 40.20; H, 4.89; N, 21.65. Found: C, 40.12; H, 4.88; N, 22.09.

[(HB(pz)$_3$ VO(OC$_3$H$_7$)$_2$], VII. To a solution of $VO(Opr^i)_3$ (1.44 g; 5.83 mmol) in 20 mL of isopropanol was added 1 equiv (1.54 g) of K[HB-(pz)$_3$], and the solution was stirred for a few minutes. The solid material that developed was filtered off, redissolved in benzene, and again filtered to remove impurities. The benzene was removed under vacuum to afford the desired complex. Yield: 77% (1.80 g).

[{HB(Me$_2$pz)$_3$}VO(OR)$_2$] (R = Me, Et), VIII and IX. Method 1. To 0.56 g of [$HB(Me_2pz)_3VOCl(DMF)$] dissolved in 15 mL of absolute alcohol (MeOH or EtOH) was added 1 equiv (0.19 g) of $AgNO_3$. A fine white precipitate of AgCl formed over 30 min after which time 162 μL of DBU (1,8 diazabicyclo[5.4.0]undec-7-ene) was added, affording an orange-brown slurry. After being stirred for 15 min, the solution was filtered through Celite and chromatographed on silica gel ($MeCl_2$/MeOH 98:2 eluent). Collection of the deep orange band and recrystallization from CH_2Cl_2/MeOH afforded the desired product. Yield (methoxy derivative): 0.14 g (30%). Anal. Calcd for $C_{17}H_{28}N_6BVO_3$: C, 47.89; H, 6.57; N, 19.71. Found: C, 47.86; H, 6.51; N, 19.60. **VIII–IX** could also be prepared by method 2, the procedure for which is given for the *tert*-butoxy derivative.

[{HB(3,5-Me$_2$pz)$_3$VOCl(OR)], R = (Bu^t), X. Method 2. To 0.5 mL of dry degassed *tert*-butyl alcohol dissolved in 30 mL of diethyl ether at −78 °C was added, dropwise over 5 min, ${}^1/_2$ equiv of neat $VOCl_3$. Warming the resulting dark red-brown slurry to room temperature and stirring for 1 h yielded a clear orange solution. The solvent was removed by evaporation and the solid redissolved in 30 mL of dry methylene chloride to which was added 3.2 g (1 equiv) of K[HB(3,5-Me_2pz)$_3$]. After being stirred for 1 h, the dark orange solution obtained was concentrated and chromatographed on silica gel using CH_2Cl_2/*t*-BuOH (98:2) as an eluant. The dark orange band of product was collected, concentrated and recrystallized from hexane. Yield: 0.64 g, 25%.

Anal. Calcd for $C_{19}H_{31}N_6BO_2VCl$: C, 48.13; H, 6.62; N, 17.77; Cl, 7.5. Found: C, 48.18; H, 6.58; N, 17.75; Cl, 6.24.

[{HB(pz)$_3$}VO$_2$]$_4$, XI. The red crystals of [$HB(pz)_3VOCl(OR)$], R = Me, Et, or *t*-butyl, were treated with hot water. The slurry was heated and stirred for 1 h and then filtered. The solid red-brown product was dissolved in methylene chloride, filtered again through Celite, and concentrated. Allowing the solution to stand overnight yielded well-formed dark red-brown crystals suitable for X-ray diffraction. The air-dried crystals sent for analysis proved to be the monodichloromethane solvate trihydrate.

Anal. Calcd for $C_{36}H_{40}N_{24}B_4V_4O_8·CH_2Cl_2·3H_2O$: C, 33.58; H, 3.63; N, 25.42. Found: C, 34.14; H, 3.33; N, 25.30.

Spectroscopic and Electrochemical Measurements. Infrared spectra were obtained on a Perkin-Elmer 1600 FT-IR as KBr pellets. Room-temperature solid-state susceptibilities were measured using a Johnson-Mathey MSB-1 susceptibility balance. UV–vis spectra were obtained on either a Perkin-Elmer 553 or HP 8520 diode array spectrophotometer. Vanadium-51 NMR spectra were recorded as previously described.[13] Proton and carbon-13 NMR spectra were recorded in $CDCl_3$ and utilized either a Bruker NR80 FT-NMR or a General Electric QE-300 spectrometer. Electrochemical data were taken on a BAS CV-27 voltammograph. Cyclic voltammograms were obtained at a Pt bead electrode in solutions containing 1 M tetrabutylammonium hexafluorophosphate as a supporting electrolyte. All potentials are referenced to the saturated calomel electrode (SCE) and employed ferrocene as an internal standard.

EXAFS Analysis. EXAFS spectra of [{HB(3,5-Me_2pz)$_3$}VO(OMe)$_2$] and [{HB(3,5-Me_2pz)$_3$}VO(OC_6H_4Br)$_2$] were recorded at the SERC Daresbury Synchrotron Radiation Source, operating at an energy of 2 GeV. The samples were prepared by grinding to a fine powder in a pestle and mortar, and mounted in thin aluminium sample holders with Sellotape windows. Data were collected in transmission mode in station 7.1, using a double crystal Si(*111*) monochromator, detuned to give 50% rejection of the incident beam in order to reduce harmonic contamination. Two scans were recorded and averaged with the source operating in multibunch, at an average current of 150 mA. Reference spectra were taken of the edge region of a 5 μm vanadium foil in order to calibrate the spectra. The spectra were background subtracted and normalized by fitting polynomials to the preedge and the postedge regions. The data were analyzed in the program EXCURV90 utilizing single- and multiple-scattering curved wave theory.[14] Phase shifts were calculated in the program, using Xα potentials and the program default values for the muffin tin radii and ionicity. Theoretical fits were generated by defining shells of backscatterers expected from the known crystal structure of the *p*-OC_6H_4Br complex[2] and then iterating the distances, *R*, and the Debye–Waller factors, $2\sigma^2$, to give the best agreement with the experimental spectra. The numbers of backscatterers were not iterated. Inclusion of multiple scattering effects from the pyrazolyl rings improved the final fit for both the OMe and the *p*-OC_6H_4Br complexes.

X-ray Data Collection and Analysis. Crystals of **I**, **V**, **VI**, **X**, and **XI** were mounted in Lindeman capillaries and transferred to either a Siemans R3mv or P4 diffractometer. Preliminary diffractometer data and axial photography led to unit cell choices. Following accurate centering of 20–25 relatively high angle reflections, intensity data were collected. Crystal data and data collection parameters are summarized in Table 1. Absorption corrections were applied to **I** (face indexed numerical method) **XI** (ψ-scan), and **V**, **VI**, and **X** (empirical, using the program XABS[15]).

Solution and Refinement of the Structures. Data were reduced and models refined by using the SHELX program package provided with the Siemans diffractometers. Structures were solved using direct methods procedures and were refined by full-matrix least-squares. Parameters used in the solution and refinement of the structures are summarized in Table 1. Hydrogen atoms were generally initially placed at idealized positions and refined isotropically riding on their respective carbon atoms except for **I** where hydrogens were refined independently. Final atomic parameters for **I**, **V**, **VI**, **X**, and **XI** are found in Tables 2–6.

(11) Trofimenko, S. *J. Am. Chem. Soc.* **1967**, *22*, 6288.
(12) Trofimenko, S. *Inorg. Synth.* **1970**, *12*, 99.
(13) Butler, A.; de la Rosa, R.; Zhou, Q.; Jhanji, A.; Carrano, C. J. *Inorg. Chem.* **1992**, *31*, 5072.
(14) (a) Binsted, N.; Campbell, J. W.; Gurman, S. J.; Stephenson, P. C. SERC Daresbury Laboratory EXCURV90 program. 1990. (b) Lee, P. A.; Pendry, J. B. *Phys. Rev.*, **1975**, *B11*, 1795. (c) Gurman, S. J.; Binsted, N.; Ross, I. *J. Phys. Chem.* **1984**, *17*, 143. (d) Gurman, S. J.; Binsted, N.; Ross, I. *J. Phys. Chem.* **1986**, *19*, 1845. (e) Blackburn, N. J.; Strange, R. W.; McFadden, L. M.; Hasnain, S. S. *J. Am. Chem. Soc.* **1987**, *109*, 7162.
(15) Walker, N.; Stuart, D. *Acta Crystallogr., Sect. A* **1983**, *39*, 158.

Table 1. Summary of Crystallographic Data and Data Collection

param	I	V	VI	X	XI
formula	$C_{20}H_{34}BCl_3N_7O_2V$	$C_{12}H_{17}BClN_6O_2V$	$C_{13}H_{19}BClN_6O_2V$	$C_{19}H_{30}BClN_6O_2V$	$C_{38}H_{44}B_4Cl_4N_{24}O_{10}V_4$
space group	$P2_1/c$	*Pbca*	*Pbca*	$P2_1/n$	*Pccn*
temp, K	198	298	298	298	298
a, Å	17.189(2)	13.361(3)	12.783(3)	8.615(2)	15.634(3)
b, Å	10.039(2)	14.583(3)	15.312(3)	17.761(4)	16.202(3)
c, Å	16.618(3)	18.016(4)	18.843(4)	16.139(3)	24.406(5)
β, deg	103.039(12)			104.58(3)	
V, Å^3	2793.9(8)	3510.2(13)	3688.1(14)	2389.9(9)	6182(2)
d_{calcd}, g cm^{-3}	1.361	1.417	1.399	1.311	1.489
Z	4	8	8	4	4
fw	572.6	374.5	388.5	471.7	1385.8
cryst size, mm	0.2 × 0.3 × 0.3	0.6 × 0.4 × 0.3	0.4 × 0.4 × 0.2	0.6 × 0.4 × 0.2	0.6 × 0.3 × 0.3
μ (cm^{-1})	6.6	7.3	7.0	5.5	8.3
radiation	graphite-monochromated Mo Kα (λ = 0.710 73 Å)				
scan type	ω	θ–2θ	θ–2θ	θ–2θ	θ–2θ
data collcn range, deg	$4.0 < 2\theta < 50.0$	$5.0 < 2\theta < 4.50$	$3.5 < 2\theta < 55.0$	$3.5 < 2\theta < 45.0$	$3.5 < 2\theta < 45.0$
No. unique data	4938	2268	2388	5423	3996
No. of obs. data(4σ(F))	2793	1432	1596	1813	2042
data to param ratio	6.5:1	6.6:1	7:4:1	6.7:1	5.3:1
transm factors	0.85/0.89	na	na	na	0.28/0.49
R[a]	5.54	5.74	4.19	7.70	7.80
R_w[b]	5.30	6.82	5.16	8.03	9.17
max diff peak, e/Å^3	0.49	0.44	0.42	0.54	0.55
Δ/σ	0.33	0.001	0.001	0.001	0.021

[a] Quantity minimized $\sum w(F_o - F_c)^2$. $R = \sum||F_o - F_c||/\sum F_o$. [b] $R_w = [\sum(w[F_o - F_c]^2/\sum(wF_o)^2)]^{1/2}$.

Table 2. Atomic Coordinates (×10^4) and Equivalent Isotropic Displacement Coefficients (Å^2 × 10^3) for I

	x	y	z	U(eq)[a]
V	2015(1)	1276(1)	668(1)	27(1)
Cl	2429(1)	3527(2)	908(1)	45(1)
B(1)	2001(4)	−244(7)	−1045(4)	30(2)
N(2)	1409(2)	921(4)	−1189(2)	23(1)
N(3)	1308(3)	1685(4)	−532(2)	27(2)
C(4)	786(3)	2654(5)	−848(3)	29(2)
C(5)	564(3)	2512(6)	−1701(3)	30(2)
C(6)	961(3)	1427(5)	−1900(3)	29(2)
C(7)	508(5)	3671(9)	−322(5)	42(3)
C(8)	924(5)	806(7)	−2729(4)	41(3)
N(9)	2842(2)	303(4)	−687(3)	28(2)
N(10)	3016(3)	883(4)	90(3)	30(2)
C(11)	3800(3)	1197(6)	257(3)	39(2)
C(12)	4111(4)	844(7)	−421(4)	45(2)
C(13)	3501(4)	284(6)	−999(3)	39(2)
C(14)	4216(5)	1866(11)	1034(5)	57(3)
C(15)	3504(5)	−273(10)	−1839(5)	60(3)
N(16)	1784(2)	−1214(4)	−412(2)	26(1)
N(17)	1804(3)	−786(5)	378(2)	29(2)
C(18)	1695(3)	−1877(6)	806(3)	30(2)
C(19)	1615(4)	−2978(6)	301(3)	34(2)
C(20)	1677(3)	−2540(5)	−453(3)	29(2)
C(21)	1682(6)	−1812(8)	1708(4)	45(3)
C(22)	1604(5)	−3305(7)	−1243(4)	45(3)
O(23)	1204(2)	1336(4)	1215(2)	33(1)
C(24)	399(4)	953(8)	982(4)	48(3)
O(25)	2786(2)	745(4)	1780(2)	36(1)
C(26)	2657(4)	1119(6)	2457(3)	37(2)
N(27)	3109(3)	807(5)	3176(3)	38(2)
C(28)	2920(6)	1219(9)	3953(4)	54(3)
C(29)	3821(5)	9(10)	3233(4)	76(4)
C1(1A)	4488(2)	7604(3)	1824(1)	114(1)
C1(2A)	3986(2)	6891(3)	130(2)	144(2)
C(1A)	3710(6)	7421(16)	989(6)	126(6)

[a] Equivalent isotropic U defined as one-third of the trace of the orthogonalized U_{ij} tensor.

Table 3. Atomic Coordinates (×10^4) and Equivalent Isotropic Displacement Coefficients (Å^2 × 10^3) for V

	x	y	z	U(eq)[a]
V(1)	1509(1)	1844(1)	1525(1)	57(1)
Cl(1)	−202(1)	1693(2)	1502(1)	88(1)
O(1)	1609(4)	2303(3)	2321(2)	78(2)
O(2)	1758(3)	712(3)	1715(2)	67(2)
N(1)	1264(4)	3124(4)	971(3)	70(2)
N(2)	1766(4)	3397(4)	362(3)	62(2)
N(6)	1936(4)	1885(4)	−227(3)	51(2)
N(5)	1509(4)	1390(4)	326(3)	52(2)
N(3)	2989(4)	2141(3)	1235(3)	58(2)
N(4)	3293(4)	2479(4)	564(3)	62(2)
C(1)	725(7)	3833(6)	1191(5)	108(4)
C(2)	846(8)	4556(6)	713(6)	120(5)
C(3)	1510(7)	4282(6)	213(5)	90(4)
C(7)	1148(5)	640(5)	16(4)	64(3)
C(8)	1320(6)	634(6)	−733(4)	81(4)
C(9)	1830(5)	1438(6)	−872(4)	67(3)
C(4)	3825(6)	2007(5)	1624(4)	78(3)
C(5)	4648(6)	2236(5)	1208(6)	91(4)
C(6)	4284(5)	2539(5)	553(5)	79(3)
C(10)	1912(8)	78(7)	2313(4)	117(5)
B(1)	2480(6)	2744(6)	−18(4)	65(3)
C(11)	1597(10)	372(7)	3020(6)	225(10)
C(12A)[b]	1429(11)	−753(7)	2132(6)	163(9)
C(12B)[b]	2906(14)	−243(27)	2354(11)	99(18)

[a] Equivalent isotropic U defined as one-third of the trace of the orthogonalized U_{ij} tensor. [b] Site occupation factor for C(12A) is 0.79(2); for C(12B) it is 0.21(2).

Results

Synthesis and Characterization: Vanadium(III). Our initial approach to preparing stable vanadium(V) tripyrazolylborate alkoxides was to first synthesize vanadium(III) alkoxy complexes and allow them to air oxidize. It was expected that the "hard" alkoxide donors would stabilize the higher oxidation states making the oxidation of V(III) to V(V) extremely facile. Vanadium(III) tripyrazolylborate alkoxides were prepared via metathesis between L*VCl_2DMF and $NaOCH_3$. Unfortunately the synthesis lead to a mixture of mono- and dialkoxides which were not easily separable. Hand separation of the mixture of crystals yielded purple blocks of the monoalkoxide and blue needles of the dialkoxide. The structure of the former complex was determined by single-crystal X-ray diffraction. The monoclinic purple crystals belonged to space group $P2_1/c$, and the structure was solved by standard direct methods. Figure 1 shows the atom labeling scheme for the neutral L*VCl(OCH_3)DMF molecule. Selected bond lengths and angles are shown in Table 7. Overall the structure is similar to that of the starting material, L*VCl_2DMF.[1] The only major deviation is in the vanadium–nitrogen bond trans to the alkoxide which is significantly longer (2.19 Å) than the other two V–N bonds or those seen in the starting material, which average 2.13 Å. This is presumably a manifestation of the trans effect, commonly seen, in a somewhat more pronounced manner,

Table 4. Atomic Coordinates (×10⁴) and Equivalent Isotropic Displacement Coefficients (Å² × 10³) for **VI**

	x	y	z	U(eq)[a]
V(1)	−1489(1)	−8202(1)	−1525(1)	45(1)
Cl(1)	289(1)	−8422(1)	−1481(1)	73(1)
O(1)	−1525(3)	−7688(2)	−2283(2)	59(1)
O(2)	−1802(3)	−9261(2)	−1756(2)	54(1)
N(1)	−1148(3)	−7024(3)	−946(2)	48(1)
N(2)	−1669(3)	−6754(3)	−360(2)	52(1)
N(3)	−3027(3)	−7836(3)	−1256(2)	47(1)
N(4)	−3324(3)	−7514(3)	−612(2)	51(1)
N(5)	−1556(3)	−8688(3)	−385(2)	50(1)
N(6)	−2000(3)	−8225(3)	146(2)	53(1)
C(1)	−483(4)	−6380(3)	−1101(3)	68(2)
C(2)	−570(5)	−5699(4)	−641(3)	85(3)
C(3)	−1338(5)	−5952(4)	−181(3)	76(2)
C(4)	−3897(4)	−7914(3)	−1644(3)	59(2)
C(5)	−4742(4)	−7649(3)	−1257(3)	72(2)
C(6)	−4356(4)	−7404(3)	−607(3)	65(2)
C(7)	−1229(4)	−9440(3)	−104(3)	60(2)
C(8)	−1456(5)	−9459(4)	614(3)	75(2)
C(9)	−1949(4)	−8685(4)	750(3)	70(2)
B(1)	−2500(5)	−7349(4)	−34(3)	60(2)
C(10)	−1883(4)	−9898(3)	−2318(3)	56(2)
C(11)	−1256(7)	−10651(4)	−2078(4)	138(4)
C(12)	−1515(6)	−9540(4)	−2993(3)	105(3)
C(13)	−3013(5)	−10142(5)	−2355(3)	106(3)

[a] Equivalent isotropic U defined as one-third of the trace of the orthogonalized U_{ij} tensor.

Table 5. Atomic Coordinates (×10⁴) and Equivalent Isotropic Displacement Coefficients (Å² × 10³) for **X**

	x	y	z	U(eq)[a]
V(1)	660(2)	2137(1)	3611(1)	27(1)
Cl(1)	−667(4)	3047(2)	2682(2)	46(1)
O(1)	2429(8)	2398(4)	3616(4)	40(3)
O(2)	371(8)	2588(3)	4528(4)	33(3)
N(1)	614(10)	1473(5)	2432(5)	34(3)
N(2)	26(10)	745(5)	2364(6)	35(3)
N(3)	1412(10)	1076(5)	4164(5)	29(3)
N(4)	614(11)	423(5)	3883(5)	36(4)
N(5)	−1844(10)	1596(5)	3438(5)	32(3)
N(6)	−2132(11)	881(5)	3123(5)	36(4)
B(1)	−699(15)	401(7)	3040(8)	33(5)
C(1)	1327(14)	1589(7)	1809(7)	45(5)
C(2)	1207(16)	948(8)	1328(8)	55(5)
C(3)	417(14)	427(7)	1669(7)	42(5)
C(4)	2706(14)	892(7)	4792(7)	43(5)
C(5)	2718(15)	127(7)	4914(8)	50(5)
C(6)	1389(16)	−155(7)	4331(8)	47(5)
C(7)	−3269(13)	1868(6)	3502(7)	33(4)
C(8)	−4445(13)	1326(6)	3190(7)	40(4)
C(9)	−3700(12)	718(6)	2966(7)	33(4)
C(21)	2083(14)	2331(6)	1689(7)	54(5)
C(23)	−42(17)	−365(8)	1404(8)	81(7)
C(24)	3934(15)	1442(7)	5263(8)	63(6)
C(26)	802(16)	−953(6)	4214(8)	59(6)
C(27)	−3489(14)	2641(6)	3812(8)	60(6)
C(29)	−4381(14)	−15(7)	2608(9)	68(6)
C(10)	973(15)	3229(7)	5083(7)	45(5)
C(11)	1292(19)	2938(8)	5987(7)	87(7)
C(12)	−338(16)	3807(7)	4940(9)	84(7)
C(13)	2437(15)	3569(8)	4886(9)	87(8)

[a] Equivalent isotropic U defined as one-third of the trace of the orthogonalized U_{ij} tensor.

in the V(IV) "vanadyl" complexes where the V—N bond *trans* to the short V=O is lengthened from 2.13 to about 2.3 Å. The vanadium(III) alkoxide bond length of 1.829(4) Å is considerably shorter than the 2.086(3) Å of the V–O_{DMF} single bond or the sum of the covalent radii, suggesting significant multiple bond character even with V(III).

Electrochemistry in DMF demonstrated that the vanadium(III) monoalkoxide could be reversibly oxidized at modest potentials (+0.57 V vs SCE) as shown by its quasireversible cyclic voltammogram. Upon air oxidation the violet colored solution initially turned green and gradually darkened to brown. Although no clean products could be isolated from these air-oxidized

Table 6. Atomic Coordinates (×10⁴) and Equivalent Isotropic Displacement Coefficients (Å² × 10³) for **XI**

	x	y	z	U(eq)[a]
V(1)	2051(1)	6503(1)	1793(1)	46(1)
V(2)	1480(1)	7037(1)	3176(1)	46(1)
N(1)	405(6)	6238(6)	3106(4)	46(4)
N(2)	217(7)	5581(6)	3454(5)	53(4)
N(3)	2077(7)	5826(6)	3442(4)	44(4)
N(4)	1677(7)	5245(7)	3757(4)	47(4)
N(5)	821(7)	6266(7)	4273(5)	55(4)
N(6)	1106(7)	6968(7)	4016(4)	50(4)
N(7)	1259(6)	5415(6)	1848(4)	45(4)
N(8)	777(6)	7071(7)	1550(4)	42(4)
N(9)	1947(8)	6198(7)	941(4)	55(4)
N(10)	195(7)	6669(7)	1236(4)	54(4)
N(11)	1255(7)	5905(7)	687(4)	56(4)
N(12)	603(6)	5218(6)	1500(5)	48(4)
O(1)	2895(5)	5961(5)	1864(4)	62(3)
O(2)	911(5)	7822(5)	3082(4)	59(3)
O(3)	1768(5)	6745(5)	2489(3)	50(3)
O(4)	2500	7500	1634(5)	48(4)
O(5)	2500	7500	3354(5)	47(4)
C(1)	−528(9)	5219(8)	3310(6)	60(6)
C(2)	−826(9)	5617(11)	2846(7)	74(7)
C(3)	−255(8)	6238(8)	2729(6)	55(5)
C(4)	2199(11)	4626(10)	3839(6)	72(7)
C(5)	2967(11)	4753(9)	3580(7)	75(7)
C(6)	2867(10)	5489(10)	3330(6)	66(6)
C(7)	1050(10)	7578(11)	4365(6)	73(6)
C(8)	568(9)	6455(12)	4792(6)	72(7)
C(9)	738(11)	7280(11)	4859(7)	91(8)
C(10)	445(9)	7782(9)	1664(5)	54(5)
C(11)	−360(10)	7850(10)	1425(7)	76(7)
C(12)	−499(9)	7184(11)	1159(7)	72(7)
C(13)	1293(8)	4824(8)	2218(6)	54(5)
C(14)	705(10)	4232(10)	2109(7)	69(7)
C(15)	275(9)	4516(9)	1654(6)	60(6)
C(16)	1476(11)	5718(10)	167(6)	75(7)
C(17)	2273(12)	5953(12)	84(7)	90(8)
C(18)	2586(10)	6247(8)	553(6)	64(6)
B(1)	439(10)	5808(9)	1017(6)	49(6)
B(2)	797(9)	5420(11)	3961(7)	56(6)
C(20)	2310(24)	3917(20)	833(12)	202(18)
Cl(1)	3344(8)	3799(8)	452(7)	321(9)
Cl(2)	1471(8)	3554(7)	383(8)	317(9)
O(6)	7500	7500	2058(16)	337(29)
O(7)	2116(19)	2371(17)	1893(9)	169(22)

[a] Equivalent isotropic U defined as one-third of the trace of the orthogonalized U_{ij} tensor.

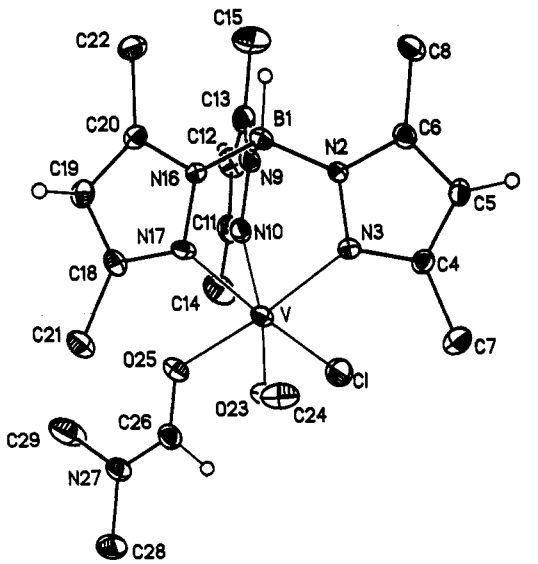

Figure 1. ORTEP diagram of L*VCl(OCH₃)DMF with 30% thermal ellipsoids showing the atom labeling scheme.

Table 7. Selected Bond Lengths (Å) and Angles (deg) for I

V–Cl	2.376(2)	V–N(3)	2.128(4)
V–N(10)	2.186(5)	V–N(17)	2.138(5)
V–O(23)	1.829(4)	V–O(25)	2.086(3)
Cl–V–N(3)	93.5(1)	Cl–V–N(10)	90.6(1)
N(3)–V–N(10)	87.9(2)	Cl–V–N(17)	171.2(1)
N(3)–V–N(17)	86.8(2)	N(10)–V–N(17)	80.6(2)
Cl–V–O(23)	96.8(1)	N(3)–V–O(23)	97.0(2)
N(10)–V–O(23)	170.9(2)	N(17)–V–O(23)	91.9(2)
Cl–V–O(25)	89.3(1)	N(3)–V–O(25)	173.7(2)
N(10)–V–O(25)	86.4(2)	N(17)–V–O(25)	89.6(1)
O(23)–V–O(25)	88.3(1)		

mixtures we believe, on the basis of the optical spectra, that the green species represents a vanadyl complex which is then further oxidized to a brown vanadium(V) alkoxo species. Numerous attempts to isolate clean vanadium(V) alkoxides by controlled oxidation of the V(III) precursors were unsuccessful. This necessitated an alternative synthesis of the desired V(V) complexes.

Vanadium(V) Synthesis and Structure. The second synthetic approach involved oxidation of V(IV) precursors in the presence of the desired alcohol. In this case, L*VOCl(DMF) was treated with $AgNO_3$ in methanol or ethanol. Initially, the solutions turned blue-violet and precipitated AgCl. Following the addition of a nonnucleophilic base to promote deprotonation of the alcohol, the solution turned a deep red brown and precipitated vanadium(V) bis(alkoxide) complexes. Presumably the mechanism involves abstraction of the halide from LVOCl(DMF) by silver ion and coordination of the alkoxide ion, followed by oxidation of V(IV) to V(V) by excess silver yielding the desired product. Unfortunately the yields for this reaction were poor, leading us to seek a better synthesis. The most obvious approach, i.e. direct reaction of $VOCl_3$ with $K[HB(pz)_3]$, had been abandoned early on due to extensive decomposition of the ligand by the vanadium oxychloride. However, we have subsequently found that the $VOCl_3$ can be reacted first with an alcohol to produce what is likely to be $VOCl(OR)_2$, which then cleanly reacts with $K[HB(pz)_3]$ to give (tripyrazolylborato)vanadium(V) alkoxo complexes. With the unsubstituted ligand all the isolated complexes were monoalkoxo, monochloro species of the form LVO(Cl)OR except when vanadium(V) isopropoxide was used as a vanadium source, which gave the bis isopropoxide derivative. With the 3,5-dimethyl-substituted ligand, bis(alkoxides) were obtained when R = Me or Et while monoalkoxo–monochloro species were obtained when R = isopropyl or *tert*-butyl. The nature of the alkoxide products in the 3,5-dimethylpyrazole series are explicable based on simple steric considerations. Only the smaller alkoxides, $-OCH_3$ and $-OCH_2CH_3$, can form bis complexes with the sterically crowded 3,5-dimethyl-substituted ligand, while the bulky *tert*-butoxy ion only allows formation of the mono-substituted species. Attempts to prepare either the corresponding monomethoxy monochloro or di-*tert*-butoxy complexes met with failure.

Although no X-ray structure is available, NMR spectra clearly show the presence of a plane of symmetry in solutions of the bis alkoxide complexes (Tables 8 and 9). The correspondence in the NMR data for the bis(alkoxides) and those of the previously structurally characterized bis(phenoxides) unambiguously establishes the structure of the former as well.[2] The monoalkoxo complexes are not expected to have a plane of symmetry; hence, each of the pyrazole rings can be unique. This leads to a more complex NMR pattern (Tables 8 and 9). The monoalkoxy–monochloro species are also chiral molecules; hence, the hydrogens on the methylene residue of the mono ethoxy and the methyls of the isopropoxy derivative of the unsubstituted pyrazolylborates are diastereotopic and readily observed by NMR. Carbon-13 NMR data on all complexes is also available as supplementary material.

The structures of several of the monoalkoxy–monochloro complexes have been determined by single-crystal X-ray diffraction studies. Orthorhombic orange crystals of $[\{HB(pz)_3\}VOCl(O\text{-}Pr^i)]$ (V) belonged to the centrosymmetric space group *Pbca* (determined unambiguously from systematic absences), with the analogous *tert*-butoxy derivative **VI** being nearly isomorphous. Since these molecules should be chiral and yet crystallize in a centrosymmetric space group there must be equivalent numbers of right and left handed forms present i.e. they crystallize as the racemic mixture. Figure 2 shows the atom labeling scheme for the neutral molecule of **V**, with selected bond lengths and angles summarized in Table 10.[16]

The V(V) is coordinated to the nitrogens of the pyrazolylborate ligand in the expected tridentate fashion with a chloride ion, the oxo group, and the alkoxo oxygen rounding out the distorted octahedral coordination sphere. As expected, the V(V) to alkoxo oxygen bond is short (1.719(4) Å), indicative of considerable multiple bond character. Indeed the $V–O_{alkoxo}$ bond is only ca. 0.1 Å longer than the formal double bond of the oxo group. The trans effect is again evident, as it is in all the vanadium(IV) or vanadium(V) tripyrazolylborates studied thus far, with the V–N bond trans to the oxo group at 2.26 Å as compared to the V–N bond trans to the chloride of 2.09 Å. Also evident is a modest trans effect for the alkoxo oxygen with V–N bond trans to it measuring 2.142 Å. Similar results are seen for the *tert*-butoxy derivative, **VI** (Figure 3), and the 3,5-dimethylpyrazolylborate *tert*-butoxy complex, **X** (Figure 4). Selected bond lengths and angles are given in Table 10.

Stability and Hydrolysis Products. The vanadium(V) alkoxide complexes prepared in this study display varying stabilities, but two trends are obvious: (1) As we have shown previously, the 3,5-dimethylpyrazolylborate complexes are kinetically considerably more stable than their unsubstituted counterparts.[3] For example, while clean ^{51}V NMR spectra can be obtained for all the 3,5-dimethylpyrazolylborates (*vide supra*), the unsubstituted complexes invariably show a multitude of signals except in the *tert*-butoxy case. In addition, while the former species are stable in storage for months, the latter decompose within days. (2) The more bulky alkoxides lead to the most stable complexes with either ligand. Thus the most stable member of either series is L*VO(*t*-butoxy)Cl. All of the complexes were found to undergo hydrolysis in the presence of water. Heating a wet acetonitrile solution of $L*VO(OCH_3)_2$ produced a red-brown species which maintained its V(V) oxidation state. The optical NMR and IR spectra of this material matched that of the previously reported hydrolysis product of $L*VO(phenoxide)_2$.[2] The hydrolysis reaction can be followed for the 3,5-dimethylpyrazolyl complexes by ^{51}V NMR. Addition of 25–50% H_2O to an acetonitrile solution of **X** resulted in a loss of the −560 ppm NMR peak with concommitant growth of a new peak at −580 ppm. The same peak is seen for all the hydrolyzed $L*VO(alkoxide)_2$, $L*VO(phenoxide)_2$, or L*VO(alkoxide)Cl complexes. Although crystalline material could be produced for the hydrolysis products involving the 3,5-dimethylpyrazolylborate ligand, rapid loss of solvent resulted in samples that were too poorly diffracting to be of use. However, on the basis of NMR, mass spectral, resonance Raman, and IR analysis, an oxo-bridged dimer seems likely.

Treatment of the alkoxide complexes of the unsubstituted tripyrazolylborate ligand with a large excess of water also resulted in their rapid hydrolysis to oxo-bridged multinuclear species. Examination of the complexes by both ^{13}C and ^1H NMR revealed the presence of 2-fold symmetry in the molecule of the hydrolysis product. Assignments of the proton NMR spectra were based on integration and COSY experiments while those of the ^{13}C were based on chemical shifts and intensities (supplementary material). Structures consistent with both the NMR and the uncharged nature of the complex include, among others, a

(16) Note the isopropyl group in V is disordered. It was modeled by placing C12 at two positions, C12a, 0.79(2) occupancy, refined anisotropically, and C12b, 0.21(2) occupancy, refined isotropically.

Table 8. ^{1}H NMR Spectral Data for $LVO(OR)_2$ and $LVO(OR)Cl$ (L = 3,5-Dimethylpyrazolylborate)

	3,5-dimethylpyrazole										
R	pyrazole C—H on "other" rings	pyrazole C—H on ring trans to V=O	"down" methyls				"up" methyls	"down" methyl on ring trans to V=O	alkoxy C—H	methyls	
dimethoxy	5.67(2)	5.61(1)	2.56(6)		2.25(9)		2.14(3)	5.09(3)			
diethoxy	5.71(2)	5.67(1)	2.60(6)		2.30(9)		2.25(3)	5.69(2)	1.36(2)		
isopropoxy-Cl	5.69(3)		2.66(3)	2.45(3)	2.37(3)		2.28(9)	3.40(1)	1.86(3)	1.21(3)	
tert-butyl-Cl	5.70(2)	5.65(1)	2.67(3)	2.44(3)	2.40(3)	2.30(6)	2.27(3)	1.85(9)			

Table 9. ^{1}H NMR Spectral Data for the Complexes $LVO(OR)Cl$ and $LVO(OR)_2$ (L = Unsubstituted Tripyrazolylborate)

	pyrazole-hydrogens (ppm)				alkoxy hydrogens		
R	down H on ring trans to V=O	down H on other	up H's on all rings	center H on all rings	C—H	methyl	
isopropyl–Cl	8.26 (1)[a]	7.89(2)	7.61(3)	6.19(3)	7.24(1)	1.75(3)	1.45(3)
methyl–Cl	8.27 (1)	7.95(2)	7.63(3)	6.24(3)	6.13(3)		
ethyl–Cl	8.24 (1)	7.90(2)	7.61(3)	6.22(3)	6.762(2)	1.62(3)	
tert-butyl–Cl	8.34 (1)	7.81(2)	7.61(3)	6.21(3)		1.86(9)	
diisopropyl	8.07 (3)		7.58(3)	6.16(3)	5.96(2)	1.45(6)	1.34(6)

[a] Numbers in parentheses represent relative integrated intensity.

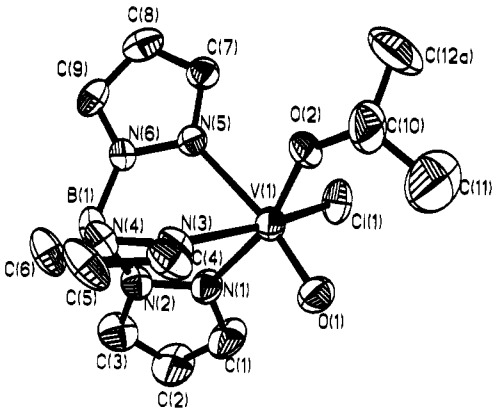

Figure 2. ORTEP diagram of $LVOCl(OPr^i)$ showing 30% thermal ellipsoids and the atom labeling scheme.

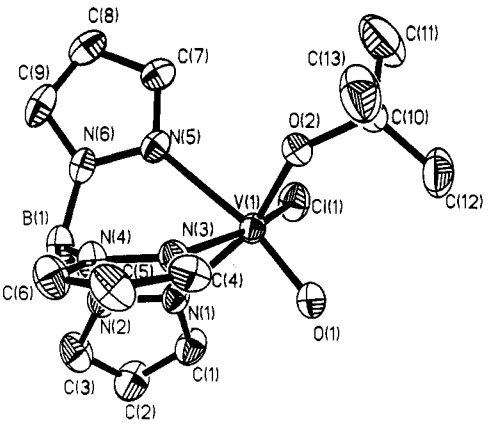

Figure 3. ORTEP diagram of $LVOCl(OBu^t)$ with 30% thermal ellipsoids showing the atom labeling scheme.

Table 10. Selected Bond Lengths (Å) and Angles (deg)

	V	VI	X
V(1)–Cl(1)	2.297(2)	2.299(2)	2.303(3)
V(1)–O(1)	1.587(5)	1.631(3)	1.592(8)
V(1)–O(2)	1.719(4)	1.726(3)	1.754(7)
V(1)–N(1)	2.142(6)	2.153(4)	2.231(9)
V(1)–N(3)	2.090(6)	2.106(4)	2.116(9)
V(1)–N(5)	2.259(5)	2.274(4)	2.313(9)
Cl(1)–V(1)–O(1)	98.1(2)	97.4(1)	96.7(3)
O(1)–V(1)–O(2)	102.1(2)	103.1(2)	101.6(3)
O(1)–V(1)–N(1)	93.8(2)	92.5(2)	88.3(4)
Cl(1)–V(1)–N(3)	163.1(2)	162.4(1)	161.6(2)
O(2)–V(1)–N(5)	84.7(2)	85.6(1)	88.0(3)
Cl(1)–V(1)–N(5)	87.4(1)	87.5(1)	85.3(2)
N(3)–V(1)–N(5)	79.8(2)	79.9(1)	81.8(3)
Cl(1)–V(1)–O(2)	96.0(2)	95.8(1)	94.4(2)
Cl(1)–V(1)–N(1)	85.6(2)	84.5(1)	85.2(2)
O(2)–V(1)–N(1)	163.6(2)	164.2(1)	170.0(3)
O(1)–V(1)–N(3)	93.4(2)	93.2(2)	93.8(4)
N(1)–V(1)–N(3)	81.2(2)	81.0(1)	80.0(3)
O(10)–V(1)–N(5)	170.7(2)	169.5(2)	169.9(4)
N(1)–V(1)–N(5)	79.0(2)	78.7(1)	82.0(3)
O(2)–V(1)–N(3)	93.8(2)	95.4(2)	98.3(3)

dihydroxy-substituted monomer, $LVO(OH)_2$, a μ-oxo–hydroxo species, $[LVO(OH)]_2O$, or the bis(μ-oxo)-bridged $[LVO_2]_2$. Fortunatey the complex yielded well-formed crystals suitable for X-ray analysis which allowed a definitive assignment of the structure. The deep red blocky crystals grown from CH_2Cl_2 were orthorhombic and belonged to space group *Pccn*. Figure 5 shows the atom labeling scheme for the asymmetric unit with selected bond lengths and angles summarized in Table 11. Not shown are the solvent molecules (one CH_2Cl_2 and one H_2O/asymmetric unit). The relatively poor *R* factors of GOF criteria are a result

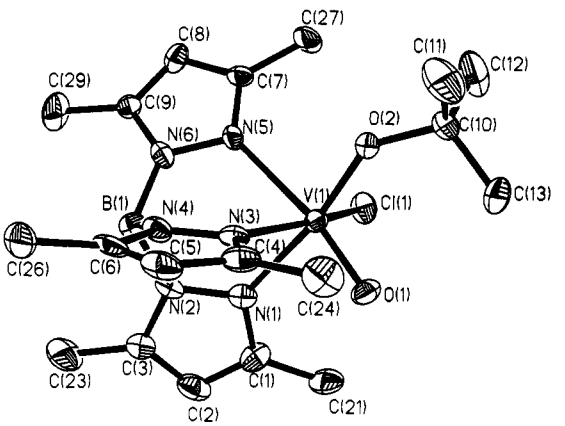

Figure 4. ORTEP diagram of $L^*VOCl(OBu^t)$ showing 30% thermal ellipsoids and the atom labeling scheme.

of our inability to come up with a completely satisfactory model for the disordered solvent molecules. One methylene chloride per asymmetric unit was indicated by both analysis and ^{1}H and ^{13}C NMR and could be modeled reasonably well. The disordered H_2O molecules sitting on or near special positions were particularly troublesome. The model ultimately chosen placed one full water molecule on a crystallographically imposed 2-fold axis with the other disordered across another 2-fold axis. Despite the disorder there can be no doubt as to the basic structure of the molecule of interest. The asymmetric unit consists of a μ-oxo-bridged dimer where each vanadium(V) is coordinated to a tridentate hydridotripyrazolylborate unit and has one terminal oxo functionality and the vanadiums are linked together by an oxo bridge

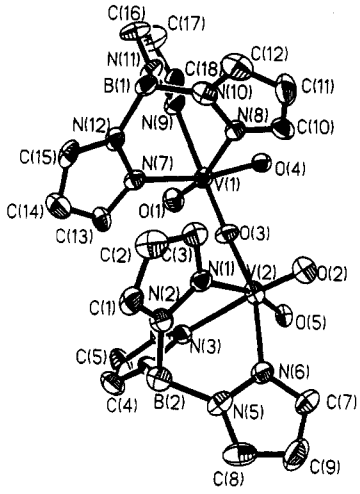

Figure 5. ORTEP diagram of the asymmetric unit of $[L_2V_2O_4]_2$ showing 30% thermal ellipsoids and the atom labeling scheme.

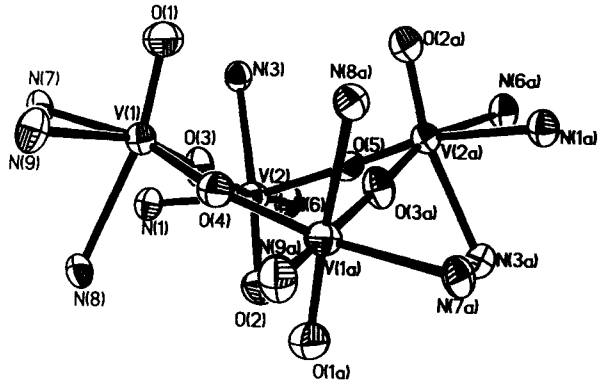

Figure 6. ORTEP diagram showing the core structure of $[L_2V_2O_4]_2$ and the coordination environment around the vanadium centers.

Table 11. Selected Bond Lengths (Å) and Angles (deg) for **XI**

V(1)–N(7)	2.159(10)	V(1)–N(8)	2.273(10)
V(1)–N(9)	2.144(11)	V(1)–O(1)	1.594(9)
V(1)–O(3)	1.798(8)	V(1)–O(4)	1.803(3)
V(2)–N(1)	2.112(10)	V(2)–N(3)	2.267(10)
V(2)–N(6)	2.134(10)	V(2)–O(2)	1.569(9)
V(2)–O(3)	1.800(8)	V(2)–O(5)	1.815(3)
N(7)–V(1)–N(8)	81.1(4)	N(7)–V(1)–N(9)	80.1(4)
N(8)–V(1)–N(9)	76.9(4)	N(7)–V(1)–O(1)	91.0(4)
N(8)–V(1)–O(1)	167.6(4)	N(9)–V(1)–O(1)	92.3(5)
N(7)–V(1)–O(3)	88.7(4)	N(8)–V(1)–O(3)	86.7(4)
N(9)–V(1)–O(3)	161.4(4)	O(1)–V(1)–O(3)	102.8(4)
N(7)–V(1)–O(4)	165.5(4)	N(8)–V(1)–O(4)	86.7(3)
N(9)–V(1)–O(4)	91.6(5)	O(1)–V(1)–O(4)	101.2(3)
O(3)–V(1)–O(4)	96.0(4)	N(1)–V(2)–N(3)	79.7(4)
N(1)–V(2)–N(6)	80.1(4)	N(3)–V(2)–N(6)	78.0(4)
N(1)–V(2)–O(2)	91.9(4)	N(3)–V(2)–O(2)	167.6(4)
N(6)–V(2)–O(2)	91.5(4)	N(1)–V(2)–O(3)	87.9(4)
N(3)–V(2)–O(3)	86.4(4)	N(6)–V(2)–O(3)	161.8(4)
O(2)–V(2)–O(3)	102.6(4)	N(1)–V(2)–O(5)	164.7(4)
N(3)–V(2)–O(5)	86.2(3)	N(6)–V(2)–O(5)	91.9(5)
O(2)–V(2)–O(5)	101.4(3)	O(3)–V(2)–O(5)	96.4(4)

involving O(3). Also bound is an additional oxygen (O(5) on V(2) and O(4) on V(1)), which sits on a crystallographically imposed 2-fold axis. This leads to the generation of a symmetry equivalent dimer molecule. Hence the overall unit (Figure 6) is a tetranuclear oxo-bridged cluster. The V_4O_4 core is not planar but adopts a butterfly configuration. The two V–O–V angles within the core are markedly different with V(1)–O(3)–V(2) nearly linear at 177.4(6)° while V(1)–O(4)–V(1a) is bent at 152.4(7)°. This leads to vanadium–vanadium distances of 3.52 Å for V(1)–V(1A) and 3.60 Å for V(1)–V(2). A number of V_4O_4 tetranuclear cores have been reported; however, most of these contain tetrahedral V(V) and hence have V–O–V bond angles between 120 and 140°.[17] A tetranuclear oxo-bridged cluster with octahedral V(V) has also been reported by Crans *et al.*[18] whose V–O–V angles average near 104°.

Table 12. ^{51}V NMR Data[a]

ppm (relative to $VOCl_3$)	complex
−588	L*VO(*p*-nitrophenoxy)$_2$
−559	L*VOCl(O-*t*-butyl)
−557	L*VO(phenoxy)$_2$
−533	L*VO(OEt)$_2$
−525	L*VO(OCH$_3$)$_2$
−484	L*VO(*p*-methoxyphenoxy)$_2$
−580[b]	L*VO(OH)$_2$
−572	LVOCl(O-*t*-butyl)
−694	$[LVO_2]_4$

[a] Unless otherwise noted solvent is CH_2Cl_2. L* = hydridotris(3,5-dimethylpyrazolylborate). L = hydridotripyrazolylborate. [b] Acetonitrile/H_2O.

Vanadium-51 NMR. Many of the complexes in this study showed relatively sharp ^{51}V NMR resonances in the range −480 to −700 ppm relative to $VOCl_3$ (Table 12). Solvent effects were small as were the effects of going from mono- to bis(alkoxides). The unsubstituted pyrazolylborate complexes were generally unstable in solution, rapidly turning from red to green. Thus only the LVO(*t*-butoxy)Cl complex showed a single species in solution. It is clear that coordination of alkoxide ligands by themselves does not lead to unusual ^{51}V NMR parameters which are in the range of most mono- or dioxo V(V) species with a wide variety of ligands.[19] Thus one will need to look elsewhere to explain the ca. −1200 ppm shift of the V(V) reported for the bromoperoxidase enzyme.[20] Pecoraro *et al.* have shown that the ^{51}V NMR shifts can be moved over a very wide range for structurally similar species when the ligands are redox noninnocent such as the catechols etc.[21] Still, the most negative shift reported for a non-organometallic vanadium complexes is the *ca.* −700 ppm for peroxo complexes.

Electrochemistry. In acetonitrile, methylene chloride, and DMF most of the alkoxo complexes displayed more or less irreversible, reductive electrochemistry. The 3,5-dimethylpyrazolylborate complexes are, as expected, more difficult to reduce than their unsubstituted counterparts. The nature of the R group in the alkoxide appears to be unimportant. The bis(alkoxide) complexes are also more difficult to reduce than the corresponding mono(alkoxide)–monochloro species. This is in line with expectations, since the good π-donating alkoxo groups should stabilize the oxophilic V(V) state better than does chloride. Indeed one can tune the redox potential of these vanadium tripyrazolylborate complexes over at least 1.5 V, providing another gratifying example of the stabilization of high oxidation states by hard ligands.

The electrochemistry of the dimethoxy complex L*VO(OCH$_3$)$_2$ was examined in some detail and can be considered typical. In CH_2Cl_2 a reduction wave is observed at −0.96 V with only a very small return reoxidation at −0.40 V, $i_{pa}/i_{pc} \approx 0.1$. A product wave (as determined by its absence if the initial scan is in the positive direction) appears at +0.45 V upon scanning through the reduction wave (Figure 7). Presumably in the reduced V(IV) state the alkoxides are not strongly bound and are lost, leading to irreversible behavior. However if the electrochemistry is run in methanol as a solvent, a quasi-reversible wave appears ($E°$ =

(17) (a) Fuchs, J.; Mahjour, S.; Pickardt, J. *Angew. Chem., Int. Ed. Engl.* **1976**, *15*, 374. (b) Day, V. W.; Klemperer, W. G.; Yagasaki, A. *Chem. Lett.* **1990**, 1267.
(18) Crans, D. C.; Marshman, R. W.; Gottlieb, M. S.; Anderson, O. P.; Miller, M. M. *Inorg. Chem.* **1992**, *31*, 4939.
(19) Rehder, D.; Weidemann, C.; Duch, A.; Priebsch, W. *Inorg. Chem.* **1988**, *27*, 584.
(20) Vilter, H.; Rehder, D. *Inorg. Chim. Acta* **1987**, *136*, L7.
(21) Cornman, C. R.; Colpas, G. J.; Hoeschele, J. D.; Kampf, J.; Pecoraro, V. L. *J. Am. Chem. Soc.* **1992**, *114*, 9925.

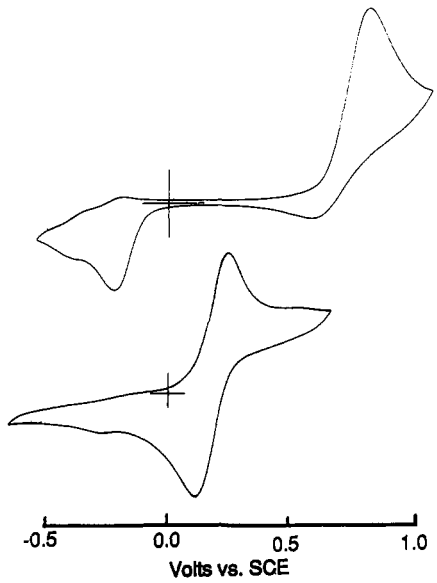

Figure 7. Cyclic voltammograms of (top) $LVO(OCH_3)_2$ in CH_2Cl_2 (bottom) $LVO(OCH_3)_2$ in CH_3OH (v = 300 mV/s; other conditions as described by the text).

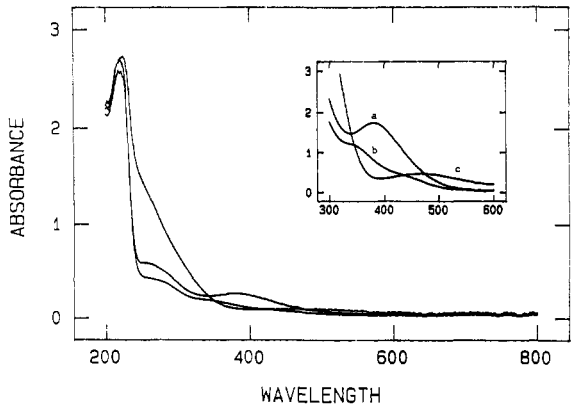

Figure 8. Optical spectra of (a) L*VO(OBu^t)Cl, (b) L*VO$(OCH_3)_2$ in CH_2Cl_2, and (c) $[L^*VO(OH)]_2O$ in CH_3CN.

–0.26v, ΔE_p = 140 mv, i_{pa}/i_{pc} = 0.75). Addition of a trace of base (tetraethylammonium hydroxide) leads to an even more reversible wave at –0.255 V ($i_{pa}/i_{pc} \approx 1.0$). The large excess of methanol/methoxide serves to keep the complex intact in both oxidation states, yielding reversible electrochemistry.

The complex $[LVO(O)]_4$ was also examined electrochemically, and surprisingly it displayed quasi-reversible electrochemistry in CH_2Cl_2 solution. A wave at $E°$ = 0.025v ($i_{pa}/i_{pc} \approx 0.7$, ΔE_p = 130 mV, ferrocene 120 mV) appears as well as two smaller product waves at +0.40 and +0.87 V. Attempts to prepare the one-electron-reduced product by bulk electrolysis were unsuccessful, however, as the product was unstable on the bulk electrolysis time scale.

Optical Spectra. All of the complexes in this study give rise to red to yellow solutions in dichloromethane and other organic solvents. These colors arise from modestly intense transitions in the blue region of the visible spectrum in the near-UV region (Figure 8). The three highest energy bands are nearly invariant in all the samples and are thus attributed to internal π–π^* transitions of the polypyrazolylborate group. The lowest energy transition (see inset) in sensitive to the nature of the complex and is assigned as a LMCT transition from a pπ orbital on the alkoxide oxygen to the empty d orbitals of the d^0 V(V). The intensity of these transitions ($\epsilon_m \approx$ 450–2000) is in accord with this assignment. The general trend in energy of this LMCT band is dialkoxy > monochloro monoalkoxy > bis(μ-oxo). It should be noted that native bromoperoxidase displays a similar optical spectrum in the near-UV region with a shoulder at ~320 nm.[22] Clearly the bis(alkoxide) spectrum is the closest match although the nature of the spectrum does not lend itself to unambiguous comparisons. The broad transitions of the oxo-bridged dimers near 450 nm appear characteristic of the V–O–V unit and have been reported previously.[23]

Table 13. Vanadium *K*-Absorption Edge Data for $[\{HB(3,5\text{-}Me_2pz)_3\}VO(OR)_2]$ (R = Me, C_6H_4-4-Br) Compared with Bromperoxidase

sample	ΔPEF,[a] eV	ΔE,[b] eV	I[c]	$v^{1/2}$,[d] eV
$[\{HB(3,5\text{-}Me_2Pz)_3\}VO(OMe)_2]$	5.7	8.7	40	2.5
$[\{HB(3,5\text{-}Me_2pz)_3\}VO(OC_6H_4Br)_2]$	5.4	8.9	35	2.3
native BPO	4.0	8.0	63	1.8
native BPO + H_2O_2	4.0	8.1	59	1.7
native BPO + Br^-	3.9	7.8	75	1.8
reduced BPO	3.1	5.7	34	2.4

[a] Shift in energy of the pre-edge feature, relative to the energy of the preedge feature of vanadium foil (≡5466.0 eV); estimated uncertainty ±0.02 eV. [b] Shift in edge position measured as the energy at half the edge height after normalization and calibration against a vanadium foil spectrum where the edge energy is taken as 5473.5 eV; estimated uncertainty ±0.04 eV. [c] Intensity of preedge feature expressed as the percentage height of the preedge feature relative to the normalized edge height; estimated uncertainty ±15%. [d] Width of preedge feature at half-maximum height.

EXAFS. Vanadium *K*-edge X-ray absorption spectra were recorded for two of the compounds prepared in this series, to provide a basis for a reevaluation of the data recorded for bromoperoxidase. The compounds studied were $[\{HB(3,5\text{-}Me_2pz)_3\}VO(OMe)_2]$ and $[\{HB(3,5\text{-}Me_2pz)_3\}VO(OC_6H_4Br)_2]$. The latter compound, the X-ray crystallographic characterization of which was reported previously,[2] was chosen to check the reliability of the analytical procedures used to analyze the EXAFS data recorded for bromoperoxidase. The former compound was chosen as we were unable to obtain crystals suitable for X-ray crystallography.

Table 13 summarizes the details of the preedge and vanadium *K*-absorption edge for the two compounds studied in this work and provides a comparison with the corresponding information for bromoperoxidase samples.[8] The edge positions of $[\{HB(3,5\text{-}Me_2pz)_3\}VO(OMe)_2]$ and $[\{HB(3,5\text{-}Me_2pz)_3\}VO(OC_6H_4Br)_2]$ are found at a rather high energy as compared with values identified previously for other vanadium(V) compounds.[8] The energy of the preedge feature has been correlated with oxidation state or more generally with the concept of coordination charge.[24] Clearly the coordination charge approach fails with these model compounds since it predicts that vanadium bound to six highly electronegative oxygen donors should have a larger coordination charge and hence a higher energy preedge feature than a vanadium bound (as if the case in these models) to three oxygen and three less electronegative nitrogen atoms. More work is needed, but speculation as to the nature of the coordination environment in vanadium species based on correlations of coordination charge and the preedge energy are clearly risky.[25]

The intensity of the preedge feature has been correlated with coordination geometry and average bond distances around the vanadium.[24] In this regard the data on the models suggests that the vanadium in bromoperoxidase either has a coordination number lower than 6 or shorter vanadium ligand bonds (or both). The general similarity in metal–ligand bond lengths for the models

(22) Tromp, M. G. M.; Olafsson, G.; Krenn, B. E.; Wever, R. *Biochim. Biophys. Acta* **1990**, *1040*, 192.
(23) (a) Kanamori, K.; Ookubo, Y.; Ino, K.; Kawai, K.; Michibata, H.; *Inorg. Chem.* **1991**, *30*, 3832. (b) Chandrasekhar, P.; Bird, P. N. *Inorg. Chem.* **1984**, *23*, 3677. (c) Money, J. K.; Folting, K.; Huffman, J. C.; Christou, G. *Inorg. Chem.* **1987**, *26*, 944.
(24) (a) Wong, J.; Lytle, F. W.; Messmer, R. P.; Maylotte, D. H. *Phys. Rev.* **1984**, *B30*, 5596. (b) Hallmeier, K. H.; Szargan, R.; Werner, G.; Meier, R.; Sheromov, M. A. *Spectrochim. Acta* **1986**, *42*, 841.

Table 14. Comparison of Crystal Structure and EXAFS Parameters for the Pyrazolylborate Models

		$VO(OC_6H_4Br)_2\{HB(Me_2pz)_3\}$					$VO(OCH_3)_2\{HB(Me_2pz)_3\}$ EXAFS		
		cryst struct		EXAFS					
ligand	atom type	N	R, Å	N	R, Å	$2\sigma^2$, Å^2	N	R, Å	$2\sigma^2$, Å^2
terminal oxide	O	1.0	1.579	1.0	1.60	0.011	1.0	1.58	0.005
$2OC_6H_4$ (or $2OCH_3$)	O	2.0	1.822, 1.857 (av 1.840)	2.0	1.84	0.012	2.0	1.77	0.007
	N	3.0	2.088, 2.119, 2.311 (av 2.173)	3.0	2.14	0.022	3.0	2.18	0.011
	N	3.0	3.065, 3.089, 3.220 (av 3.125)	3.0	3.12	0.015	3.0	3.12	0.015
pyrazole groups	C	3.0	3.008, 3.151, 3.361 (av 3.173)	3.0	3.20	0.014	3.0	3.20	0.014
	C	3.0	4.238, 4.260, 4.412 (av 4.303)	3.0	4.25	0.030	3.0	4.31	0.034
	C	3.0	4.269, 4.304, 4.501 (av 4.358)	3.0	4.39	0.030	3.0	4.39	0.035
	B	1.0	3.314	1.0	3.25	0.001	1.0	3.34	0.013
$2OC_6H_4$ (or $2OCH_3$)	C	2.0	2.894, 3.050 (av 2.972)	2.0	3.08	0.001	2.0	3.08	0.013
$2CH_3 + C_6H_4$ (or $3CH_3$)	C	3.0	3.314, 3.498, 3.542 (av 3.551)	3.0	3.41	0.016	3.0	3.51	0.010
$1CH_3 + 1C_6H_4$	C	2.0	3.688, 3.746 (av 3.717)	2.0	3.68	0.016			
$2C_6H_4$	C	2.0	4.118, 4.152 (av 4.135)	2.0	4.25	0.012			

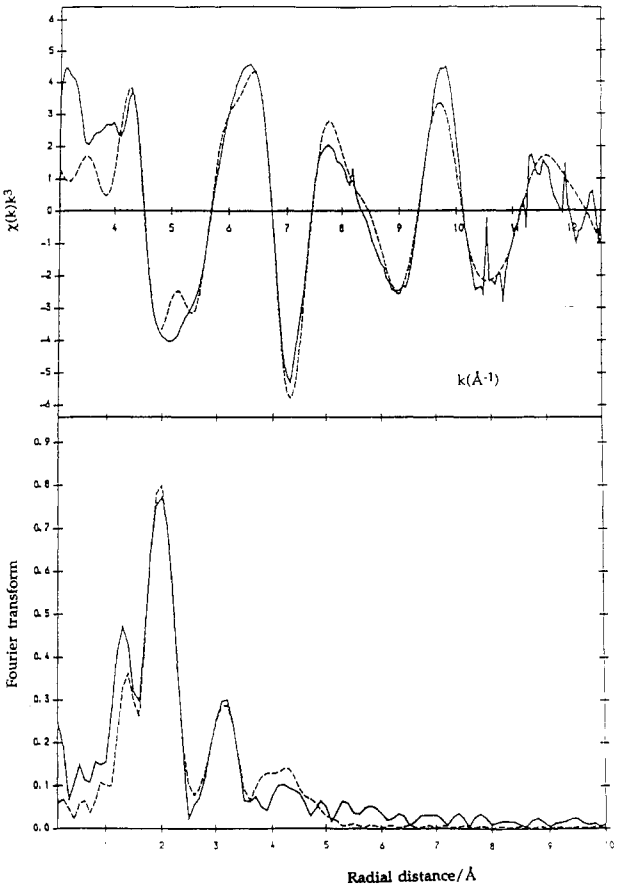

Figure 9. Vanadium K-edge EXAFS (xk^3) of $[\{HB(3,5\text{-}Me_2pz)_3\}VO(OMe)_2]$ and associated phase-corrected Fourier transform: (—) experimental data; (- - -) simulation using the parameters given in Table 14.

as compared to those determined for bromoperoxidase by EXAFS would seem to favor the former possibility. Overall, the edge profile suggest that the nature of the vanadium environment in these compounds is *not* identical to the environment of the metal in native bromoperoxidase.

The EXAFS associated with the vanadium K-absorption edge has been extracted and analyzed (Figure 9). The metal–ligand distances required to interpret the EXAFS recorded for $[\{HB(3,5\text{-}Me_2pz)_3\}VO(OC_6H_4Br)_2]$ (Table 14) are, given the large numbers of shells involved, in good agreement with the crystallographic values[2] and give confidence in using the procedure to obtain the metal–ligand distances for $[\{HB(3,5\text{-}Me_2pz)_3\}VO(OMe)_2]$ (Table 14) and bromoperoxidase. The geometrical relationships within the pyrazole rings required the use of multiple scattering. The three pyrazole rings were treated as a single unit, and the five shells were included initially at the average crystallographic distances in $[\{HB(3,5\text{-}Me_2pz)_3\}VO(OC_6H_4Br)_2]$ and their backscattering contributions refined as one group. Each of the outer shells was only included in the EXAFS analysis if its contribution was statistically significant.[26] These studies suggest that the V–OMe distances are significantly (*ca.* 0.1 Å) shorter than the $V\text{–}OC_6H_4Br$ distances. It is noteworthy that

Table 15. X-ray Crystallographic Data for Known Vanadium(V) Alkoxide Complexes

V = O, Å	$V\text{—}O_{alkoxide}$, Å	complex[c]	ref
1.54	1.740	$VO(OMe)_3$	27
1.584	1.767	$VO(OCH_2CH_2Cl)_3$	28
1.595	1.763	$VO(cyclo\text{-}C_5H_9O)_3$	29
1.576	1.773	$[VO(pinacol)Cl]_2$	30
1.585	1.773	VO(CPS)(OEt)	31
1.598	1.805	$[VO(SALAHE)]_2$	32
1.600	1.774	$VO(HQ)(O^ipr)$	33
1.612	1.783	$[(tacn)_2V_2O_2(OH)_2(\mu\text{-}O)]^{2+}$	34
1.586	1.764	VO(HPS)(OEt)	31
1.614	1.819	VO(pentan-3-olsal$_2$)	35
1.595	1.750	VO(BH)(OEt)	36
1.591	1.803	VO(HHD)O^{i}pPr)	37
1.579	1.778	VO(Sal-L-ala)(OCH_3)	38
1.589	1.754	$(VOCl)_2(VO(OH))_2(DMPD)_4$	18
1.630	1.726	$HB(pz)_3VO(O\text{-}Bu^t)Cl$	this work
1.597	1.719	$HB(pz)_3VO(O\text{-}Pr^i)Cl$	this work
1.595	1.754	$HB(3,5\ Me_2Pz)_3VO(O\text{-}Bu^t)Cl$	this work
1.58	1.77[b]	$HB(3,5\ Me_2pz)_3VO(OCH_3)_2$	this work
1.589	1.776 ± 0.016[a]	mean	

[a] Not including the four values from this work. [b] From EXAFS. [c] Key: CPS = carboxyphenylsalicylidenaminato; SALAHE = 2-(salicylideneamino)-1-hydroxyethanato; HQ = 8-hydroxyquinolinato; TACN = 1,4,7-trimethyl-1,4,7-triazacyclononane; HPS = hydroxyphenylsalicylidenaminato; pentan-3-olsal$_2$ = *N,N*-(3-hydroxypentanyl)bis(salicylaldiminato); BH = 4-phenylbutane-2,4-dionylbenzoylhydrazonato; HHD = *N,N'*-dihydroxy-*N,N'*-diisopropylheptandiamido; Sal-L-ala = *N*-salicylidene-L-alaninato; DMPD = 2,2-dimethyl-1,3-propanediol.

(25) Weidemann, C.; Rehder, D.; Kuetgens, U.; Hormes, J. *J. Chem. Phys.* **1989**, *136*, 405.
(26) Joyner, R. W.; Martin, K. J.; Meehan, P. *J. Phys. Chem.* **1987**, *20*, 4005.
(27) Caughlan, C. N.; Smith, N. M.; Watenpaugh, K. *Inorg. Chem.* **1966**, *12*, 2131.
(28) Priebsch, W.; Rehder, D. *Inorg. Chem.* **1990**, *29*, 3013.
(29) Hillerns, F.; Olbrich, F.; Behrens, U.; Rehder, D. *Angew. Chem. Int. Ed. Engl.* **1992**, *31*, 447.
(30) Crans, D. C.; Felty, R.; Miller, M. M. *J. Am. Chem. Soc.* **1991**, *113*, 265.
(31) Clague, M. J.; Keder, N. L.; Butler, A. *Inorg. Chem.* **1993**, *32*, 4754.
(32) Carrano, C. J.; Nunn, C. M.; Quan, R.; Bonadies, J. A.; Pecoraro, V. L. *Inorg. Chem.* **1990**, *29*, 944.
(33) Scheidt, W. R. *Inorg. Chem.* **1973**, *12*, 1758.
(34) Knopp, P.; Weighardt, K.; Nuber, B.; Weiss, J.; Sheldrick, W. S. *Inorg. Chem.* **1990**, *29*, 363.
(35) Dutton, J. C.; Murray, K. S.; Tiekink, E. R. T. *Inorg. Chim. Acta* **1989**, *166*, 5.
(36) Diamantis, A. A.; Frederiksen, J. M.; Salam, M. A.; Snow, M. R.; Tiekink, E. R. T. *Aust. J. Chem.* **1986**, *39*, 1081.
(37) Fisher, D. C.; Barclay-Peet, S. J.; Balfe, C. A.; Raymond, K. N. *Inorg. Chem.* **1989**, *28*, 4399.
(38) Nakajima, K.; Kojima, M.; Toriumi, K.; Saito, K.; Fujita, J. *Bull. Chem. Soc. Jpn.* **1989**, *62*, 760.

the V–OMe bond length in the bis(methoxide) as determined by EXAFS (1.77 Å) is exactly in line with expectations based on the average length of V–$O_{alkoxide}$ bonds previously reported but is considerably longer than those found for the corresponding monoalkoxo–monochloro species (*vide infra*).

Discussion

One of the unique features of the V(V) binding site in bromoperoxidase, as determined by EXAFS spectroscopy, is the presence of one or more ligand–metal bonds of ca. 1.72 Å Considerable speculation as to the nature of the ligating group(s) responsible has appeared. Candidates have included a tyrosine phenoxide, serine or threonine alkoxide or simple protonation of a V(V) oxo to a hydroxo group. In Table 15 we have compiled a list of the known V(V) alkoxide coordination complexes for which X-ray diffraction data is available. At first glance it appears that either an alkoxide or hydroxide might be a reasonable candidate as both have relatively short V–O bonds. However on closer inspection (until now) all the known alkoxide or hydroxide complexes have V–O bonds significantly longer than the 1.72 Å observed in the active form of bromoperoxidase.[8] Indeed the V–$O_{alkoxide}$ bond length clusters around 1.78 Å, or 0.06 Å longer than is observed in the EXAFS of the enzyme (there is only one hydroxo complex on the list; it has a V–O of 1.783 Å). In contrast the three pyrazolylborate monoalkoxo–monochloro complexes reported here have, to the best of our knowledge, the shortest V–O_{alkoxo} bonds yet reported (average 1.733 Å). Although the sample size is limited, there seems to be a steric effect on the V–O bond length with the least sterically demanding isopropoxide and the unsubstituted pyrazolylborate combination having the shortest, (1.719(4) Å) bond while the very sterically demanding *tert*-butoxy–3,5-dimethylpyrazolylborate combination has the longest bond of the three at 1.754(7) Å. In fact there is a clear correlation in all the coordination sphere bond lengths with steric crowding in the monochloro–monoalkoxo complexes. There also appears to be an electronic effect on the V–$O_{alkoxide}$ bond lengths as the bis(alkoxide) complexes have longer V–O bonds than the monochloro–mono(alkoxide) species. However there are not a sufficient number of the structurally characterized bis(alkoxide) complexes to test the generality of this observation.

As previously noted in the L*VO(phenoxide)$_2$ series there is also a correlation between the redox potential and both the ^{51}V NMR chemical shifts and position of the LMCT band in the alkoxide complexes reported here.[2] As expected, the easier the V(V) center is to reduce, the lower in energy the LMCT band is (which essentially involves a photoreduction of the metal). This suggests that the V(V) in bromoperoxidase is relatively difficult to reduce since its LMCT band appears as a shoulder near 315 nm.

In reexamining the EXAFS data for bromoperoxidase we were prompted to apply the bond valence sum analysis (BVS) of Thorp.[39] Briefly, bond valences are calculated according to eq 1,where r_0 and B (0.37) are empirically determined parameters or can be calculated according to simple formulas, and r is the experimentally determined bond length for a particular bond.

$$S = \exp[(r_0 - r)/B] \quad (1)$$

Values for r_0 used are listed below:

bond	r_0, Å
V^{4+}–O	1.784
V^{5+}–O	1.803
V^{4+}–N	1.874
V^{5+}–N	1.894

Given the bond length values determined by EXAFS for bromoperoxidase in both its native and reduced forms we can calculate the BVS for both native and reduced bromoperoxidase. The principal finding using this approach is that reasonable values for the known oxidation states, with the experimentally determined bond lengths, can only be obtained by assuming that the vanadium center is closer to a five-coordinate rather than six-coordinate geometry. A BVS of nearly 4.0 is determined for the reduced enzyme [known to be V(IV)] when a five-coordinate structure with one V=O bond at 1.63 Å, two V—N bonds of 2.11 Å, and two V—O bonds of 1.91 Å is considered. Likewise a value near 5.0 is obtained for the native V(V) enzyme assuming one V=O bond at 1.61 Å, two short V–O bonds at 1.72 Å and two long V—O bonds of 2.11 Å. An equally good model, within the expected accuracy of the method, can be had assuming that one of the long V–O bonds is replaced by a V–N bond. It should be noted that the bond trans to the oxo group would be expected to be very long. Hence a six-coordinate structure with a very long axial bond would also fit the BVS model (i.e. a 2.5-Å trans V–O bond would contribute only 0.15 units to the total BVS with longer bonds contributing even less). Tests of the BVS approach on a variety of vanadium model complexes suggests the method works well with vanadium in both the IV and V oxidation states.

In conclusion we have shown that vanadium(V) alkoxide bonds can be short enough to account for the 1.72-Å distance seen in the EXAFS of the native enzyme. However, simulations of the EXAFS of native bromoperoxidase based on parameters derived from the present models, indicates that they are not accurate models for the overall structure and that the number of bound imidazoles in the enzyme is two or less. Finally, the bond valence sum analysis and other data presented here are most consistent with a five-coordinate structure for both the native and reduced enzymes.

Acknowledgment. This work was supported in part by Robert A. Welch Foundation Grant AI-1157 (C.J.C.), the Texas Advanced Research Program under Grant 003615-002 (C.J.C.), and the NIH, Grant GM 38130 (A.B.). A.B. also wishes to express appreciation to the Sloan Foundation for a fellowship. Support for the purchase of the X-ray diffractometer facilities at SWT came in part from NSF-ILI Grant USE 9151286 to C.J.C. The authors also thank Dr. Vincent Lynch, Department of Chemistry, University of Texas at Austin, for the crystal structure determination of **I**, and the Director of the Daresbury Laboratory for the use of facilities.

Supplementary Material Available: Tables of ^{13}C and ^{1}H NMR data, complete bond length and angles, anisotropic displacement parameters and hydrogen atom coordinates for compounds **I**, **V**, **VI**, **X**, and **XI** (24 pages). Ordering information is given on any current masthead page.

(39) Thorp, H. H. *Inorg. Chem.* **1992**, *31*, 1585.